BJP British Journal of Pharmacology

DOI:10.1111/bph.12063
www.brjpharmacol.org

RESEARCH PAPER

Notoginsenoside R1 attenuates cardiac dysfunction in endotoxemic mice: an insight into oestrogen receptor activation and PI3K/Akt signalling

Bing Sun[1]*, Jing Xiao[1]*, Xiao-Bo Sun[1] and Ying Wu[2]

[1]*Research Center for Pharmacology and Toxicology, Institute of Medicinal Plant Development (IMPLAD), Chinese Academy of Medical Sciences & Peking Union Medical College, Beijing, China, and* [2]*Academy of Chinese Materia Medica, Wenzhou Medical College, Wenzhou, China*

Correspondence
Bing Sun and Xiao-Bo Sun, Research Center for Pharmacology and Toxicology, Institute of Medicinal Plant Development (IMPLAD), Chinese Academy of Medical Sciences & Peking Union Medical College, Beijing 100193, China. E-mail: bsun@implad.ac.cn; sunbingddd@gmail.com (SB); suntougao@gmail.com (S XB)

*These authors contributed equally to this paper.

Keywords
notoginsenoside R1; cardiac dysfunction; endotoxin; oestrogen receptor; PI3K/PKB (Akt) signalling pathway

Received
6 June 2012
Revised
10 October 2012
Accepted
13 November 2012

BACKGROUND AND PURPOSE

Notoginsenoside R1 (NG-R1), a novel phytoestrogen isolated from *Panax notoginseng*, is believed to have anti-inflammatory, anti-oxidative and anti-apoptotic properties. However, its cardioprotective properties and underlying mechanisms are largely unknown. Here we have assessed the contribution of the anti-inflammatory effects of NG-R1 to the amelioration of septic cardiac dysfunction and inflammation in mice.

EXPERIMENTAL APPROACH

We assessed cardiac function in mice by echocardiography. We studied the protein or mRNA levels of some inflammatory factors, apoptotic factors and oestrogen receptors (ERs) in heart tissues upon stimulation with bacterial LPS, NG-R1 or some pharmacological inhibitors.

KEY RESULTS

Six hours after LPS administration (10 $mg \cdot kg^{-1}$, i.p.) cardiac function was decreased, an effect attenuated by NG-R1 pretreatment (25 $mg \cdot kg^{-1} \cdot d^{-1}$, i.p.). NG-R1 also improved the imbalance between iNOS and eNOS, prevented activation of NF-κB and the subsequent myocardial inflammatory and apoptotic responses in endotoxemic mice. The effects of NG-R1 were closely associated with activation of the oestrogen receptor ERα and of PI3K/PKB (Akt) signalling, as characterized by NG-R1-induced preservation in ERα, phospho-Akt, phospho-GSK3β and I-κBα, and of cardiac function that was partially blocked by selective inhibitors of ERα or PI3K. However, NG-R1 had no effect on LPS-activated TLR-4.

CONCLUSIONS AND IMPLICATIONS

NG-R1 is a promising compound for protecting the heart from septic shock, possibly via the activation of ERα and PI3K/Akt signalling. This mechanism produces blockade of NF-κB activation and attenuation of the pro-inflammatory state and apoptotic stress in the myocardium.

Abbreviations

Akt, PKB; EF, ejection fraction; ER, oestrogen receptor; FS, fractional shortening; GSKβ, glycogen synthase kinase β; I-κBα, inhibitory-κBα; LVDd, left ventricular internal diameter at diastolic phase; LVDs, left ventricular internal diameter at systolic phase; MyD88, myeloid differentiation protein 88; NG-R1, Notoginsenoside R1

Introduction

Sepsis is a systemic inflammatory response syndrome that results from the inflammatory response of a host to infection via the activation of the innate immune system (Merx and Weber, 2007; Zanotti-Cavazzoni and Hollenberg, 2009). Sepsis is currently a major cause of mortality in hospitalized patients (Zanotti-Cavazzoni and Hollenberg, 2009). Sepsis and septic shock elicit a series of pathophysiological injuries, among which cardiac dysfunction is the most frequent cause of high mortality (Merx and Weber, 2007). Accumulating evidence suggests that the prevention of cardiac dysfunction can significantly decrease mortality in patients with sepsis (Merx and Weber, 2007; Zanotti-Cavazzoni and Hollenberg, 2009). Therefore, the search for an effective antagonist to endotoxemia-induced cardiac dysfunction remains a critical issue in both clinical and basic research (Court *et al.*, 2002).

LPS from bacterial endotoxin is a major trigger of sepsis (Rudiger and Singer, 2007). LPS can stimulate multiple cells to release a large amount of inflammatory cytokines, including TNF-α, IL-1β, IL-6, the chemokine CCL2 and the cytokine-inducible NOS (iNOS). Numerous experimental studies have shown that LPS directly act on cardiomyocytes by binding to its receptor, Toll-like receptor 4 (TLR-4) (Rudiger and Singer, 2007; Zanotti-Cavazzoni and Hollenberg, 2009; Avlas *et al.*, 2011; receptor nomenclature follows Alexander *et al.*, 2011). As a consequence, many signalling pathways, including the NF-κB pathway are activated. NF-κB is an important signal integrator that controls the production of many pro-inflammatory cytokines (Kawai and Akira, 2007; Avlas *et al.*, 2011). On the other hand, overexpressed TNF-α can trigger death receptor-induced apoptotic responses by binding to the membrane-bound TNF-α receptor 1 (TNF-R1), a well-known death receptor. The interaction leads to the activation of caspase-8, -9 and -3, inducing the apoptotic response (Wencker *et al.*, 2003).

Studies on both humans and animals have implicated the roles of oestrogen receptors (ERs) in many pathophysiological processes, including endotoxin-induced cardiac dysfunction (Hale *et al.*, 1997; Schroder *et al.*, 1998; Wu *et al.*, 2005). Clinical studies on patients with sepsis have revealed that mortality rates and TNF-α levels are lower in women than in men (Schroder *et al.*, 1998). Oestrogen replacement reduces both the myocardial infarct size and ventricular arrhythmias in rabbits (Hale *et al.*, 1997). 17β-Estradiol can reportedly reduce pathological cardiac hypertrophy and heart failure by up-regulating the PI3K/PKB (Akt) signalling pathway (Wu *et al.*, 2005). Thus, ERs and their downstream PI3K/Akt signalling pathway play important roles in limiting pro-inflammatory responses during sepsis/septic shock both *in vitro* and *in vivo*.

Panax notoginseng, also known as Sanqi, is a famous traditional Chinese herb that has long been used to treat cardiovascular diseases in China (Lei and Chiou, 1986). Notoginsenoside R1 (NG-R1), a major component and novel phytoestrogen isolated from *P. notoginseng*, is known to have anti-inflammatory, anti-oxidative and anti-apoptotic properties (Zhang *et al.*, 1997; Zhang and Wang, 2006a; Sun *et al.*, 2007; Chen *et al.*, 2008; Liu *et al.*, 2010). However, its cardioprotective properties and underlying mechanisms are largely undefined. Therefore, in the present study, we evaluated the effects of NG-R1 on cardiac dysfunction during sepsis and septic shock in mice. We observed for the first time, to the best of our knowledge, that NG-R1 significantly attenuated cardiac dysfunction in endotoxemic mice. The mechanisms by which NG-R1 attenuates cardiac dysfunction in endotoxemia involve a selective induction of ERα and preserved activation of the PI3K/Akt signalling pathway.

Methods

Animals and induction of endotoxemia

All animal care and experimental protocols were approved by the Chinese Academy of Medical Sciences & Peking Union Medical College. All studies involving animals are reported in accordance with the ARRIVE guidelines for reporting experiments involving animals (Kilkenny *et al.*, 2010; McGrath *et al.*, 2010). A total of 60 animals were used in the experiments described here. Male C57BL/6 mice 10–12 weeks old were randomly assigned to four groups. The control group (Cont; n = 15), comprised mice injected i.p. with normal saline (the solvent for LPS and NG-R1). The NG-R1 group (R1; n = 15) comprised mice treated with NG-R1 at a dose of 25 mg·kg^{-1} i.p. every day for a total of three injections. The LPS group (LPS; n = 15) comprised mice treated with LPS at a dose of 10 mg·kg^{-1} i.p. for one injection. The LPS dosage was based on previous reports that showed myocardial dysfunction without mortality (Niu *et al.*, 2008). The NG-R1 and LPS co-treatment group (R1 + LPS; n = 15) comprised mice treated with NG-R1 at a dose of 25 mg·kg^{-1} i.p. every day for a total of three injections, followed by LPS (10 mg·kg^{-1}, i.p.). Endotoxemia was induced by LPS as previously described (Niu *et al.*, 2008). At 6 h post-injection, heart tissues were fixed in 4% buffered paraformaldehyde for histology and immunohistochemistry or frozen in liquid nitrogen for RNA and protein analyses.

Determination of cardiac dysfunction by echocardiography

Mice were injected with LPS. In a separate experiment, mice were pretreated with a non-selective ER antagonist, ICI 182780 (ICI; 2 mg·kg^{-1}) (Davis *et al.*, 2008), a selective PI3K antagonist, wortmannin (1 mg·kg^{-1}) (Zhou *et al.*, 2011), or a selective ERα antagonist, methyl piperidino-pyrazole (MPP; 2 mg·kg^{-1}) (Valsecchi *et al.*, 2008) 1 h before LPS administration (n = 15 per group). The PI3K and ER inhibitor doses were chosen based on the results of previous studies (Davis *et al.*, 2008; Valsecchi *et al.*, 2008; Zhou *et al.*, 2011). The current results show no effect on cardiac function (Supporting Information Figure S2). About 6 h after LPS administration, cardiac function was examined by echocardiography using a Vevo 770 micro-ultrasound system (VisualSonics, Toronto, Ontario, Canada) as described previously (Tarin *et al.*, 2011). In brief, an *in vivo* transthoracic echocardiography of the left ventricle was performed using a 30 MHz scanhead interfaced with a Vevo 770. The ultrasound beam was placed on the heart and near the papillary muscles. High-resolution, two-dimensional electrocardiogram-based kilohertz visualization was achieved. B-mode and M-mode images were acquired and were then used to calculate the left ventricular function

parameters. A single operator who was unaware of the treatments, performed all echocardiograms. The parameters of cardiac function were measured digitally on the M-mode tracings and averaged from three to five cardiac cycles.

Histological and immunohistochemical analysis

About 6 h after LPS administration, serial sections (4 μm) of the heart tissues were taken for haematoxylin–eosin (H&E) staining or immunohistochemistry under a light microscope, as previously described (Tarin *et al.*, 2011). Briefly, myocardial leucocytes and CD11b-positive cells were counted on nine random fields on each slide with a magnification of 200×. The infiltration of myocardial leukocytes or CD11b-positive cells was expressed as the average number of leukocytes or CD11b-positive cells per field (n = 15 per group).

In situ *detection of apoptosis in heart tissue*

Cell apoptosis in heart tissue was determined by TUNEL assay using an *in situ* cell death detection kit and fluorescein (Roche Applied Science, Quebec, Canada) as previously described (Xiao *et al.*, 2012).

Western blot analysis

Heart tissues were lysed on ice with T-PER Tissue or Cell Protein Extraction Reagent (Pierce Chemical Co., Rockford, IL) containing 0.1 mM dithiothreitol and proteinase inhibitor cocktail. Lysate preparation and Western blot analysis were performed as previously described (Xiao *et al.*, 2010). The protein concentration was determined using a Bio-Rad DC Protein Determination Kit with BSA as the standard. The immunoblots were developed using an ECL kit. Six mice were included in each group.

Caspase-3, -8 and -9 activity assay

Caspase-3, -8 and -9 activities were measured using a Fluorometric Assay Kit (BioVision, Mountain View, CA, USA) according to the manufacturer's instructions. The samples were read in a Fluoroskan Ascent FL fluorometer (Thermo Fisher Scientific, Watham, MA, USA) using 400 nm excitation and 505 nm emission wavelengths, and the results were expressed as fold change over the control.

Real-time RT-PCR

Total RNA was extracted using TRIzol (Invitrogen, Carlsbad, CA). About 2 μg of total RNA was reverse transcribed using the SuperScript First-Strand Synthesis System (Invitrogen). cDNA was synthesized from the isolated RNA, and cycle time values were obtained using real-time RT-PCR with the Power SYBR Green PCR Master Mix (Applied Biosystems, Foster City, CA) as well as iQ5 Real-Time PCR Detection System and analysis software (Bio-Rad, Hercules, CA, USA) as previously described (Xiao *et al.*, 2010). The primers were designed using the Applied Biosystems Primer Express Software (version 2.0) (shown in Supporting Information Table S1). Six mice were included in each group.

Biochemical measurements

The TNF-α, IL-1β, IL-6, IFN-γ, CCL2 and IL-10 levels were quantified by ELISA according to the manufacturer's instructions (R&D Systems, Wiesbaden, Germany).

Data analysis

The data are expressed as mean ± SE. The significance of the differences between the means was assessed using the Student's t-test, and P-values less than 0.05 were considered significant. A one-way ANOVA test with Bonferroni corrections was used to determine the significance for multiple comparisons. The calculations were performed using SPSS (version 11.0) statistical software.

Materials

NG-R1 was purchased from Shanghai Winherb Medical S & T Development (Shanghai, China). The molecular structure of NG-R1 is shown in Figure 1A. All tissue culture materials were from Gibco (Grand Island, NY). All other antibodies were purchased from Santa Cruz Biotechnology (Santa Cruz, CA). All chemicals were purchased from Sigma (St. Louis, MO).

Results

Pretreatment with NG-R1 attenuated cardiac dysfunction following LPS administration

LPS-induced cardiac dysfunction was dose-dependently improved by NG-R1 treatment. A higher NG-R1 concentration (up to 50 mg·kg^{-1}) showed no additional benefit to the echocardiographic parameters. Therefore, the 25 mg·kg^{-1} dose was used in subsequent *in vivo* experiments (Supporting Information Figure S1). There was no significant difference in left ventricular functions between saline-treated and NG-R1-treated mice (Figure 1B and C). LPS administration significantly decreased the cardiac function in mice as shown by the reduction in ejection fraction (EF), fractional shortening (FS), left ventricular internal diameter at diastolic phase (LVDd) and left ventricular internal diameter at systolic phase (LVDs) compared with saline-treated controls. However, LPS-induced cardiac dysfunction was attenuated by NG-R1 pretreatment. Figure 1D shows the treatment scheme for the mice.

Pretreatment with NG-R1 protected against LPS-induced heart damage

Figure 2A and B show no apparent difference in the cardiac morphology between saline-treated and NG-R1-treated mice. However, LPS administration significantly increased erythrocyte leakage and leukocyte infiltration into the cardiac interstitium, as observed by using H&E staining (Figure 2A). Besides, CD11b-positive cells, representing polymorphonuclear neutrophils and monocyte/macrophages in an activated state (Babior, 1999), had increased within the heart after LPS challenge (Figure 2B). In contrast, NG-R1 pretreatment clearly attenuated LPS-induced neutrophil/leukocyte infiltration.

Pretreatment with NG-R1 inhibits the LPS-induced production of inflammatory cytokines by myocardium

There was no significant difference between the mRNA and protein levels of myocardial TNF-α, IL-1β and IL-6 expression in saline-treated and NG-R1-treated mice (Figure 2C and D). However, the levels of myocardial TNF-α, IL-1β and IL-6

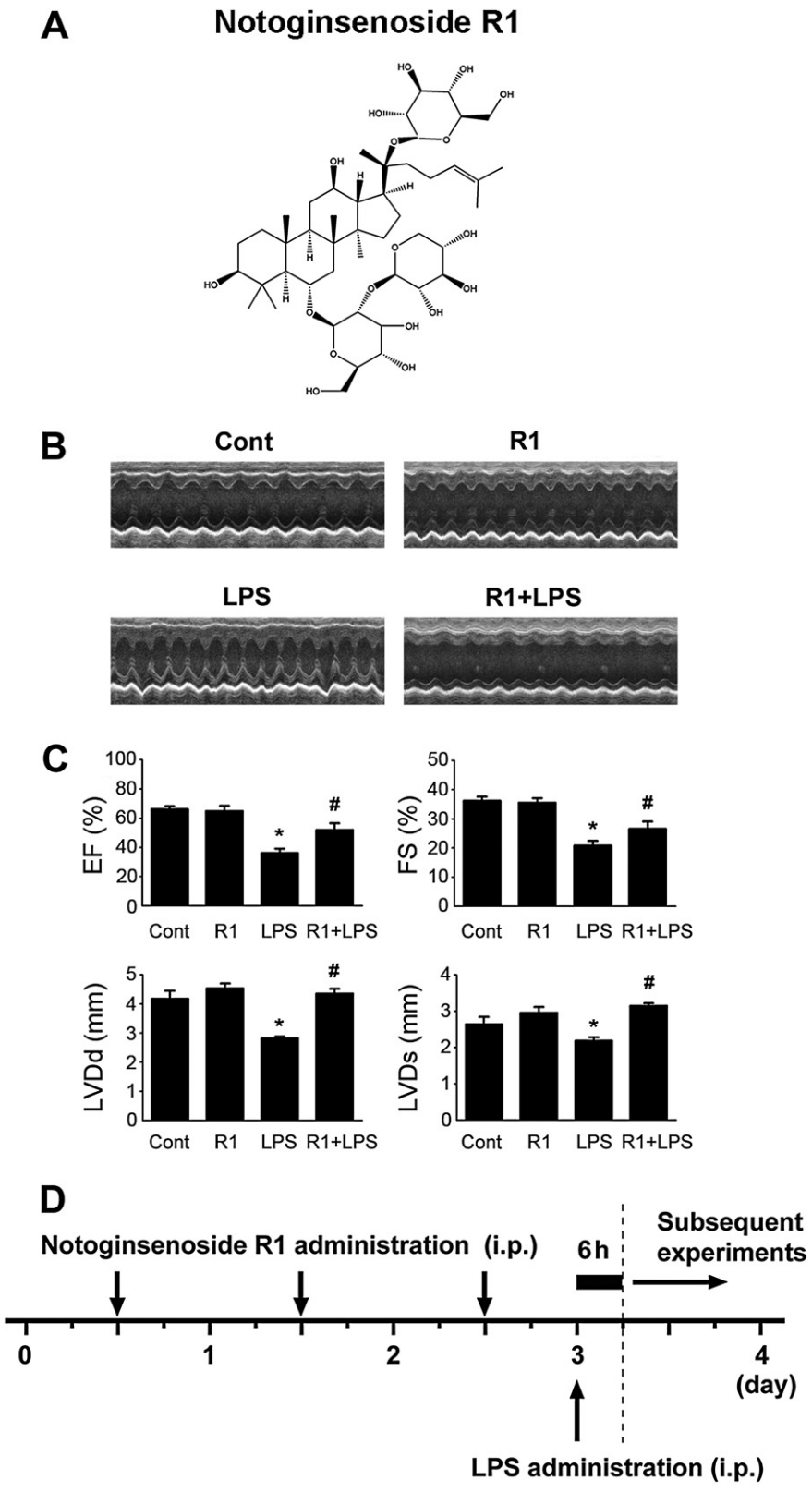

Figure 1

Effects of LPS and NG-R1 on cardiac dysfunction. (A) Molecular structure of NG-R1. (B) Mice were treated with saline or LPS (10 mg·kg^{-1}, i.p.) with or without NG-R1 pretreatment (25 mg·kg^{-1}, i.p.). Cardiac function was examined by echocardiography 6 h after LPS administration. Representative M-mode echocardiography images are shown. (C) Echocardiography values are expressed as mean ± SE (n = 15 per group). (D) Treatment scheme of the mice. *P < 0.05 versus control (Cont); $^{\#}P$ < 0.05 versus LPS-treated mice.

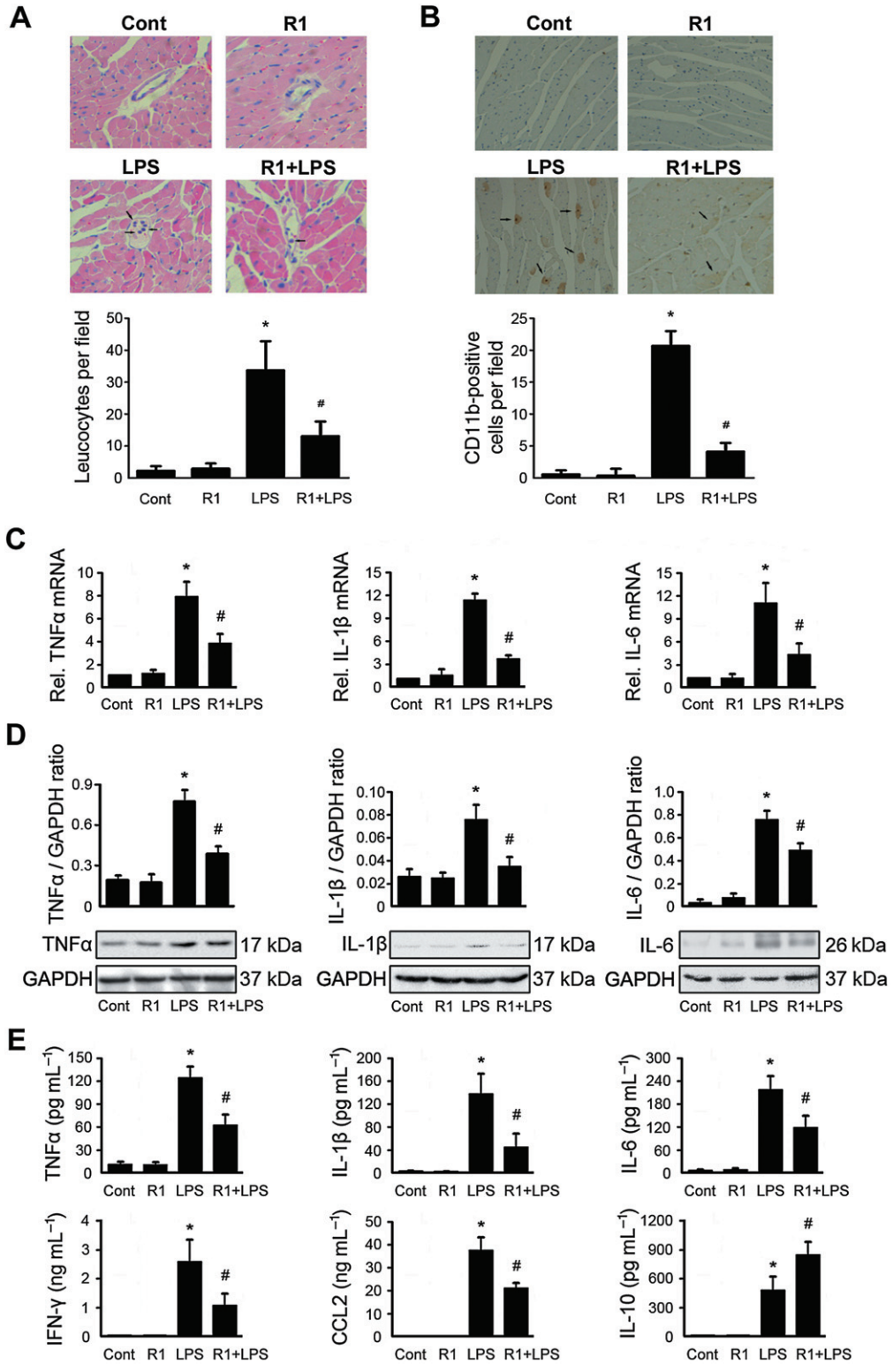

Figure 2

Effects of LPS and NG-R1 on neutrophil/leukocyte infiltration and inflammatory cytokines release. (A and B) After 6 h LPS administration, hearts were collected and sectioned for HE counterstaining (A) or immunohistochemistry (B). Infiltrated leukocytes or CD11b-positive cells were calculated. Arrowheads in panel A indicate infiltrated leukocytes; arrowheads in panel B indicate CD11b-positive cells. (C) Myocardial TNF-α, IL-1β and IL-6 expression were assayed by quantitative real-time RT-PCR ($n = 6$ per group). (D) Myocardial TNF-α, IL-1β and IL-6 expression was assayed by Western blot analysis ($n = 6$ per group). (E) The serum circulating levels of TNF-α, IL-1β, IL-6, IFN-γ, CCL2 and IL-10 were measured by ELISA ($n = 6$ per group). *$P < 0.05$ versus Cont; #$P < 0.05$ versus LPS-treated mice.

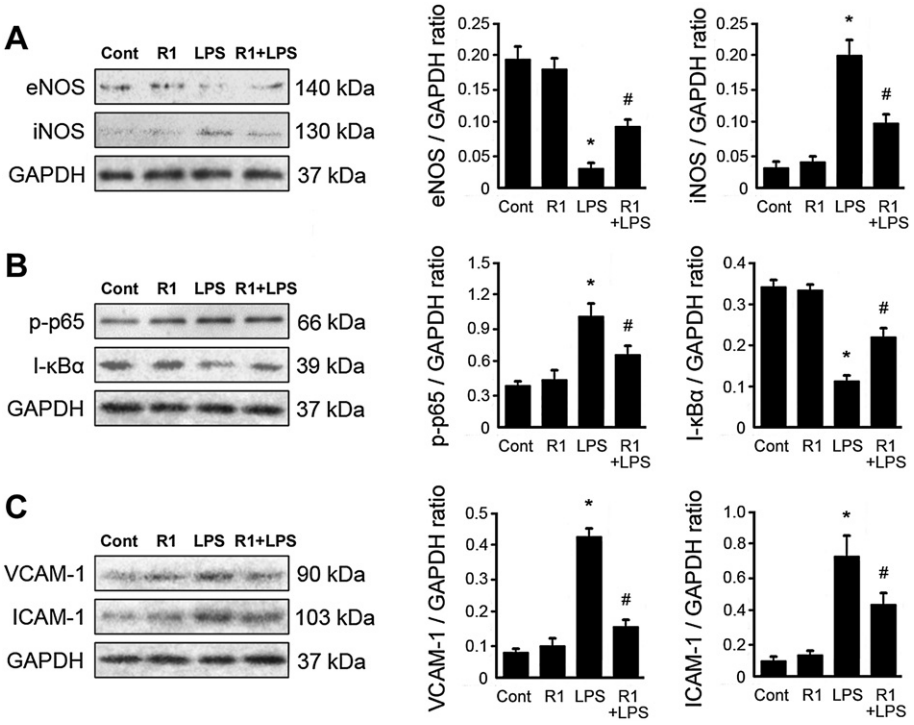

Figure 3

Effects of LPS and NG-R1 on the levels of eNOS, iNOS, VCAM-1 and ICAM-1 in heart tissues, as well as myocardial NF-κB activation (n = 6 per group). (A–C) Analysis of the protein levels of eNOS, iNOS, p-p65, I-κBα, VCAM-1 ICAM-1 and GAPDH by Western blot. For p-p65 and I-κBα examination, hearts were collected 1 h after LPS challenge. *P < 0.05 versus Cont; #P < 0.05 versus LPS-treated mice.

mRNA markedly increased after 6 h of LPS exposure compared with those of saline-treated controls (Figure 2C). This increase in myocardial TNF-α, IL-1β and IL-6 mRNA was significantly attenuated in the NG-R1 and LPS co-treatment group. This pattern of gene expression changes was also seen at the protein levels (Figure 2D), suggesting that NG-R1 pretreatment leads to the suppression of myocardial inflammatory responses during endotoxemia.

The effects of NG-R1 on LPS-induced systemic inflammatory response were measured by the serum levels of circulating inflammatory cytokines. The levels of TNF-α, IL-1β, IL-6, IFN-γ, CCL2 and IL-10 were elevated in mouse serum after 6 h of LPS exposure (Figure 2E). In contrast, NG-R1 pretreatment significantly inhibited the increase in serum TNF-α, IL-1β, IL-6, IFN-γ and CCL2 levels caused by LPS exposure. We also detected a significant stimulatory effect of NG-R1 on IL-10 levels in LPS-treated mouse serum (Figure 2E).

Pretreatment with NG-R1 attenuated the LPS-induced decrease in eNOS and increase in iNOS

An imbalance between iNOS and eNOS can contribute to the systemic hypotension and myocardial dysfunction in sepsis (Tatsumi *et al.*, 2004; Baumgarten *et al.*, 2006). As shown in Figure 3A, LPS administration significantly decreased eNOS levels, compared with those in saline-treated mice. In contrast, LPS administration did not significantly decrease eNOS levels after NG-R1 pretreatment. There was no significant difference between the protein levels of eNOS in saline-treated and NG-R1-treated mice. The iNOS levels were almost undetectable in saline-treated and NG-R1-treated mice (Figure 3A). LPS increased iNOS levels, compared with saline-treated controls, and this increase was significantly attenuated by NG-R1 pretreatment.

Pretreatment with NG-R1 attenuated LPS-induced myocardial NF-κB activation

Myocardial NF-κB is activated after cardiac dysfunction during sepsis and septic shock (Kawai and Akira, 2007). As shown in Figure 3B, there was no significant difference between the phosphorylation of the p65 subunit of NF-κB and I-κBα in the myocardium of saline-treated and NG-R1-treated mice. With 1 h LPS treatment, p65 phosphorylation significantly increased and the protein levels of I-κBα decreased compared with saline-treated controls. However, LPS-induced p65 phosphorylation and I-κBα degradation were significantly attenuated in the NG-R1 and LPS co-treatment group.

Pretreatment with NG-R1 attenuated the LPS-induced increase in myocardial VCAM-1 and ICAM-1

As shown in Figure 3C, there was no significant difference between the levels of both VCAM-1 and ICAM-1 in saline-treated and NG-R1-treated mice. However, LPS administration significantly up-regulated the protein levels of VCAM-1

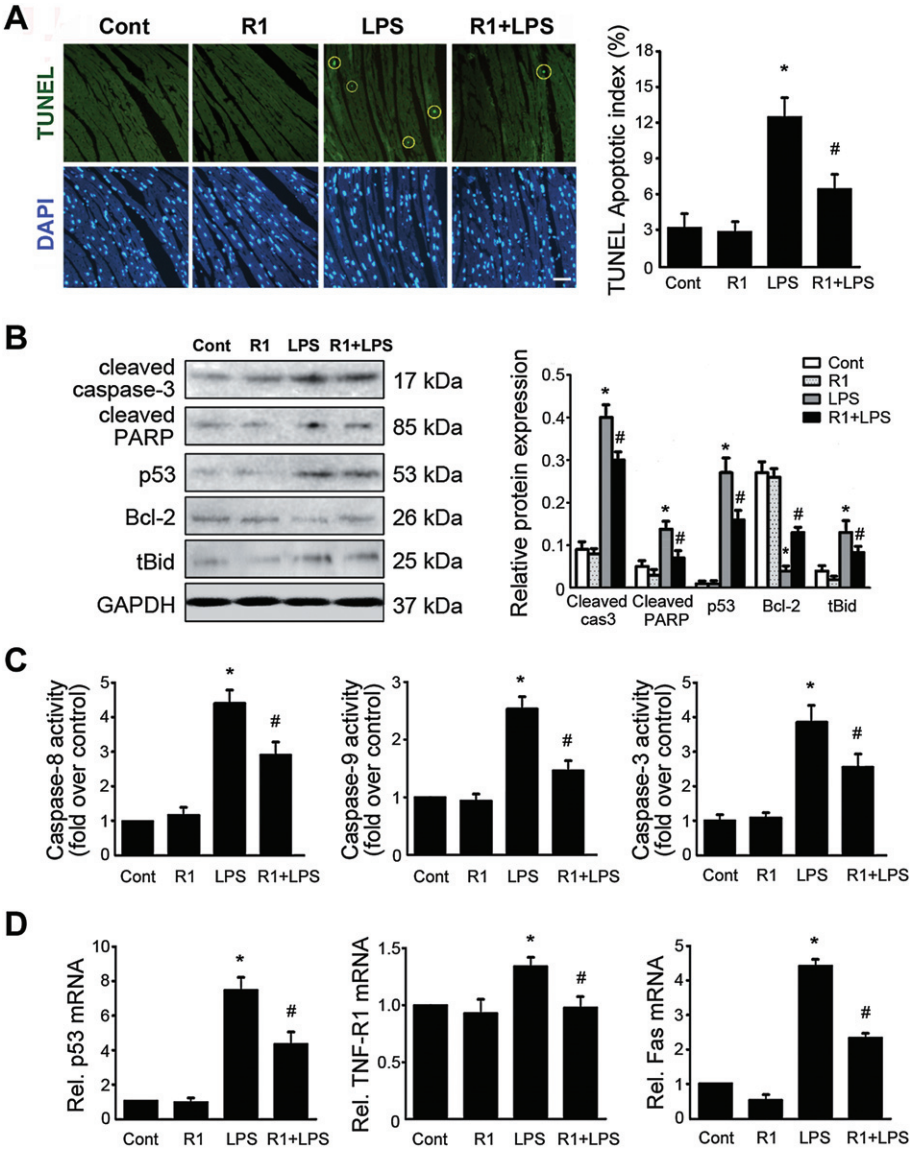

Figure 4

Effects of LPS and NG-R1 on apoptotic damage and apoptosis-related gene expression in heart tissues. (A) TUNEL assay of heart tissues (A, scale bar = 50 μm). Yellow circles in the photgraphs indicate the nuclei of apoptotic cells. The TUNEL apoptotic index was determined by calculating the ratio of TUNEL-positive cells to total cells. (B) Cleaved caspase-3, cleaved PARP, p53, Bcl-2 and t-Bid protein levels in heart tissues were determined by Western blot analysis (n = 6 per group). (C) The activities of caspase-8, -9 and -3 were measured using a fluorometric assay and expressed as the fold change over the control. (D) mRNA levels of p53, TNFR1 and Fas were determined by real-time RT-PCR (n = 6 per group). The levels of mRNA were normalized to that of GAPDH. Relative mRNA levels are shown using arbitrary units, and the value of the control group (Cont) is defined as 1. *P < 0.05 versus Cont; $^{\#}P$ < 0.05 versus LPS-treated mice.

and ICAM-1, respectively, compared with saline-treated controls. The increased protein levels of both VCAM-1 and ICAM-1 were attenuated in NG-R1 and LPS co-treated mice compared with LPS-treated mice.

Pretreatment with NG-R1 inhibits LPS-induced apoptosis and regulates apoptosis-related gene expression in the myocardium

Apoptotic damage has been implicated in cardiac dysfunction during sepsis/septic shock (Narula *et al.*, 2000). To determine whether the observed cardioprotection of NG-R1 against endotoxin-induced cardiac dysfunction was associated with apoptosis, the apoptotic index of mouse heart tissues were assessed (Figure 4A). A much larger number of TUNEL-positive cells, mainly inflammatory cells, were observed in cardiac sections from LPS-treated mice than in those from NG-R1 and LPS co-treated mice.

The activation of caspase-3, which results in the cleavage of PARP, is one of the key processes involved in apoptosis and contributes to myocardial dysfunction during sepsis/septic shock (Li *et al.*, 2009). Figure 4B shows that compared with

LPS-treated mice, myocardial caspase-3 activation was reduced in NG-R1 and LPS co-treated mice, as shown by the cleavage of caspase-3 and increased caspase-3 activity (Figure 4B and C). This change was also manifested by the reduced PARP cleavage in myocardium of NG-R1 and LPS co-treated mice (Figure 4B). LPS exposure also increased the levels of the pro-apoptotic proteins p53 and tBid, and reduced the levels of the anti-apoptotic protein Bcl-2, respectively, which was attenuated by NG-R1 pretreatment (Figure 4B). Figure 4C and D show that apoptotic damage was activated in the myocardium of LPS-treated mice, as evidenced by elevated caspase-8, -9 and -3 activities (Figure 4C), as well as increased mRNA levels in p53, TNF-R1 and Fas, which was attenuated by NG-R1 pretreatment (Figure 4D).

Pretreatment with NG-R1 attenuated the LPS-induced decrease in myocardial ERα, phospho-Akt and phospho-GSK3β

The molecular structure of NG-R1 is similar to that of oestrogens; thus, we determined whether NG-R1 pretreatment affects ERs. As shown in Figure 5A, NG-R1 selectively induced myocardial ERα expression but had no obvious effect on the ERβ levels. However, this selective induction of ERα was partially blocked by ICI 182780 (a non-selective ER antagonist) (Figure 5B). The PI3K signalling pathway, a survival regulation pathway that elicits protein kinase cascades downstream of ER activation, is also reported to play a key role in cardiac dysfunction during sepsis and septic shock (Murphy, 2011). As is shown in Figure 5A, LPS administration significantly decreased the levels of phospho-Akt, phospho-GSK3β and I-κBα compared with saline-treated controls. The levels of phospho-Akt, phospho-GSK3β and I-κBα were preserved in NG-R1 and LPS co-treated mice compared with LPS-treated mice. NG-R1-preserved expression of phospho-Akt and phospho-GSK3β was also partially blocked by ICI 182780 (Figure 5B); whereas the NG-R1-preserved expression of ERα was not inhibited by wortmannin, suggesting that PI3K/Akt may be downstream regulators of ERα in this pathophysiological process. Also, both ERα and PI3K inhibition leads to increased I-κBα degradation, suggesting that NG-R1 may attenuate LPS-induced NF-κB activation and inflammation response partially through ERα and PI3K signalling. On the other hand, NG-R1 had no obvious effect on the LPS-induced up-regulation of TLR-4. There was also no significant difference between the levels of all aforementioned genes in saline-treated and NG-R1-treated mice.

ERα or PI3K inhibition abolished the protective effect of NG-R1 on LPS-induced cardiac dysfunction

To assess further whether ERα and/or PI3K signalling was associated with the cardioprotective properties of NG-R1, we evaluated cardiac function in mice by echocardiography upon stimulation with LPS, NG-R1 or some pharmacological inhibitors. Figure 5C and D show that either non-selective (ICI 182780) or selective (MPP) antagonism of ERα, as well as selective antagonism (wortmannin) of PI3K, decreased EF, FS, LVDd and LVDs in NG-R1 and LPS co-treated mice. Importantly, these pharmacological inhibitors abolished the beneficial effect of NG-R1 on the cardiac dysfunction in LPS-induced sepsis.

Discussion and conclusions

NG-R1, a major and novel phytoestrogen isolated from *P. notoginseng*, is believed to have anti-inflammatory, anti-oxidative and anti-apoptotic properties (Zhang *et al.*, 1997; Zhang and Wang, 2006a; Sun *et al.*, 2007; Chen *et al.*, 2008; Liu *et al.*, 2010). However, its cardioprotective properties and underlying mechanisms are largely unknown. In this study, a series of experiments was designed to clarify whether the anti-inflammatory potency of NG-R1 contributed to the amelioration of septic cardiac dysfunction and inflammation in mice. The pivotal findings in the present study are as follows. (i) We observed for the first time, to the best of our knowledge, that NG-R1 significantly attenuated cardiac dysfunction in endotoxemic mice. (ii) We also observed that NG-R1 significantly inhibited LPS-induced neutrophil/leukocyte infiltration into the myocardium. (iii) Further studies indicated that NG-R1 improved the imbalance between iNOS and eNOS, reduced the VCAM-1/ICAM-1 levels, as well as preventing NF-κB activation and the subsequent myocardial inflammatory and apoptotic responses. (iv) Most importantly, the cardioprotective effects depended on the activation of ERα and pro-survival kinase PI3K.

Neutrophil/leukocyte infiltration contributes to cardiac dysfunction during sepsis/septic shock (Davani *et al.*, 2006; Muller, 2009). During this pathological process, a series of pro-inflammatory cytokines, particularly TNF-α, IL-1β, IL-6 and CCL2, is released. These cytokines are the major triggers of endotoxin-induced cardiac dysfunction (Davani *et al.*, 2006). The present study showed that LPS administration significantly deteriorated myocardial contractile function and increased neutrophil/leukocyte infiltration in the myocardium. These phenomena were accompanied by the elevated myocardial expression of a series of pro-inflammatory cytokines such as TNF-α, IL-1β, IL-6, IFN-γ and CCL2. Mast cell activation is also involved in cardiac dysfunction during sepsis and septic shock (Supporting Information Figure S4). In addition, mast cells can release injurious molecules during infection or ischemia-reperfusion to induce damaging processes in the heart (Jolly *et al.*, 1982; Frangogiannis *et al.*, 1998; Hara *et al.*, 1999; Mallen-St Clair *et al.*, 2004). On the other hand, NG-R1 inhibited all abovementioned activities induced by the LPS challenge. Our data also show that the release of anti-inflammatory IL-10 was enhanced by NG-R1 pretreatment (Figure 2). IL-10 has a crucial function in limiting inflammatory responses and preventing host damage and enhancement of IL-10 production is effective in the clinical treatment of septic shock (Saraiva and O'Garra, 2010). We also observed increased protein levels of VCAM-1 and ICAM-1 in the myocardium following LPS challenge, consistent with previous studies indicating that the LPS-increased binding of ICAM-1/VCAM-1 to the cell surface results in neutrophil/leukocyte transmigration and infiltration into the myocardium (Muller, 2009). These events lead to the increased heterogeneity of intracellular Ca^{2+} release and decreased cardiomyocyte contractility (Davani *et al.*, 2006). LPS and pro-inflammatory cytokines can up-regulate iNOS activity in cardiomyocytes and transgenic mice with the overexpression of eNOS showing a reduction in LPS-induced mortality (Yamashita *et al.*, 2000). The present study also showed that LPS administration caused an imbal-

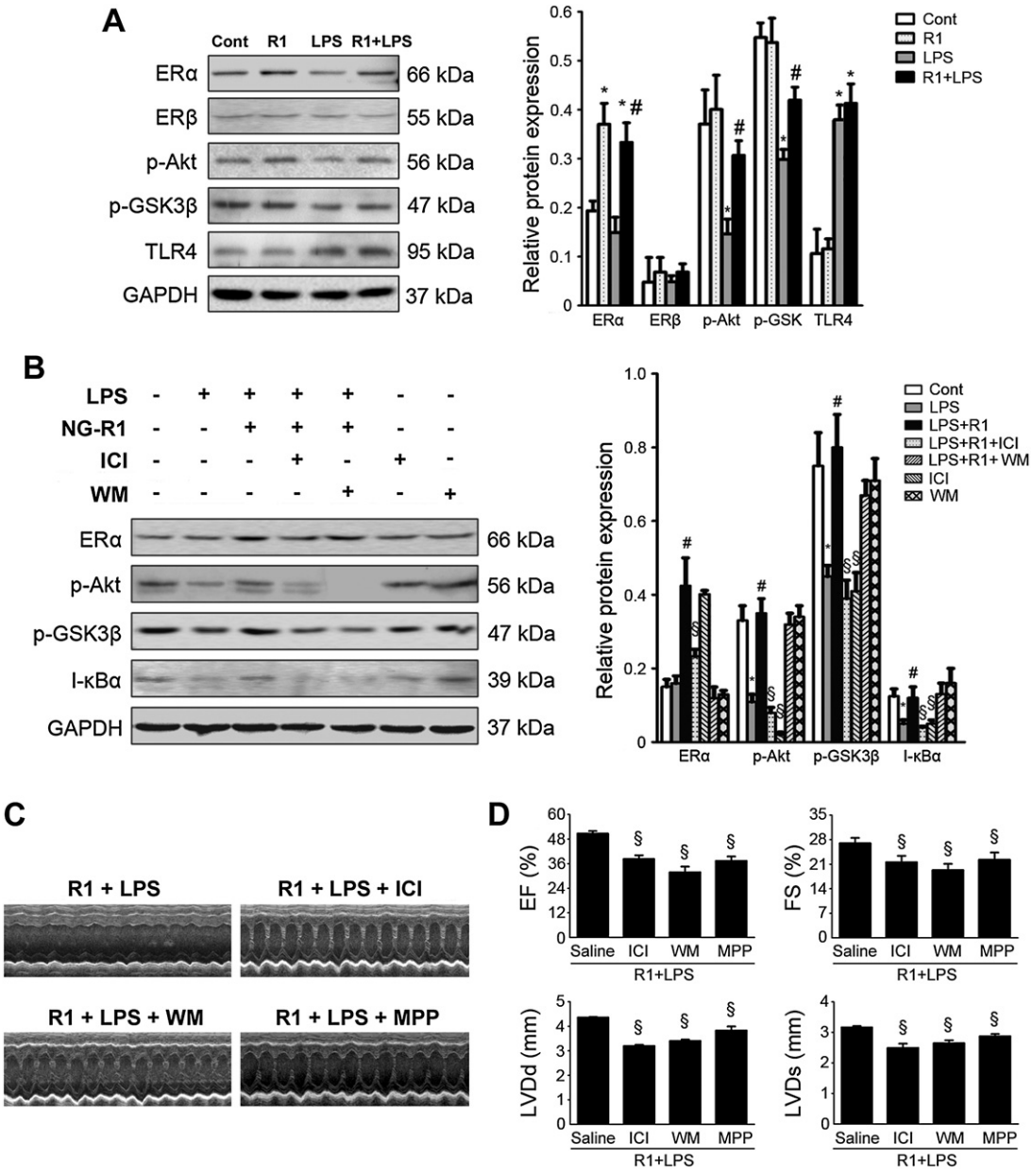

Figure 5

Involvement of ERα and PI3K/Akt signalling in LPS-induced cardiac dysfunction. (A) Protein levels of ERα, ERβ, phospho-Akt, phospho-GSK3β, and TLR4 in the myocardium examined by Western blot analysis ($n = 6$ per group). (B) Effect of a series of pharmacological inhibitors, including ICI 182780 (a non-selective ERα antagonist), wortmannin (WM, a selective PI3K antagonist) or normal saline on the levels of ERα, phospho-Akt, phospho-GSK3β, and I-κBα in the myocardium of NG-R1 and LPS co-treated mice ($n = 6$ per group). (C) Effect of a series of pharmacological inhibitors, including wortmannin (a selective PI3K antagonist), ICI 182780 (a non-selective ERα antagonist), MPP (selective ERα antagonist) or normal saline on cardiac dysfunction of NG-R1 and LPS co-treated mice. Representative M-mode echocardiography images are shown. (D) Echocardiography values are expressed as mean ± SE ($n = 15$ per group). *$P < 0.05$ versus Cont; #$P < 0.05$ versus LPS-treated mice; §$P < 0.05$ versus NG-R1 and LPS co-treated mice.

ance between eNOS and iNOS in the myocardium. This imbalance may be triggered by LPS challenge and/or pro-inflammatory cytokine overproduction (Tatsumi *et al.*, 2004), which was significantly inhibited by NG-R1 pretreatment.

LPS induces myocardial inflammation and dysfunction by interacting with its ligand TLR-4, thus triggering the activation of several signalling pathways, including the NF-κB pathway (Baumgarten *et al.*, 2006; Kawai and Akira, 2007; Avlas *et al.*, 2011). NF-κB activation is an important signal integrator controlling the production of many pro-inflammatory cytokines (Kawai and Akira, 2007). Our data confirmed that the role of myocardial inflammatory activation on myocardial dysfunction after LPS challenge was initiated by the activation of cardiac NF-κB, as demonstrated by

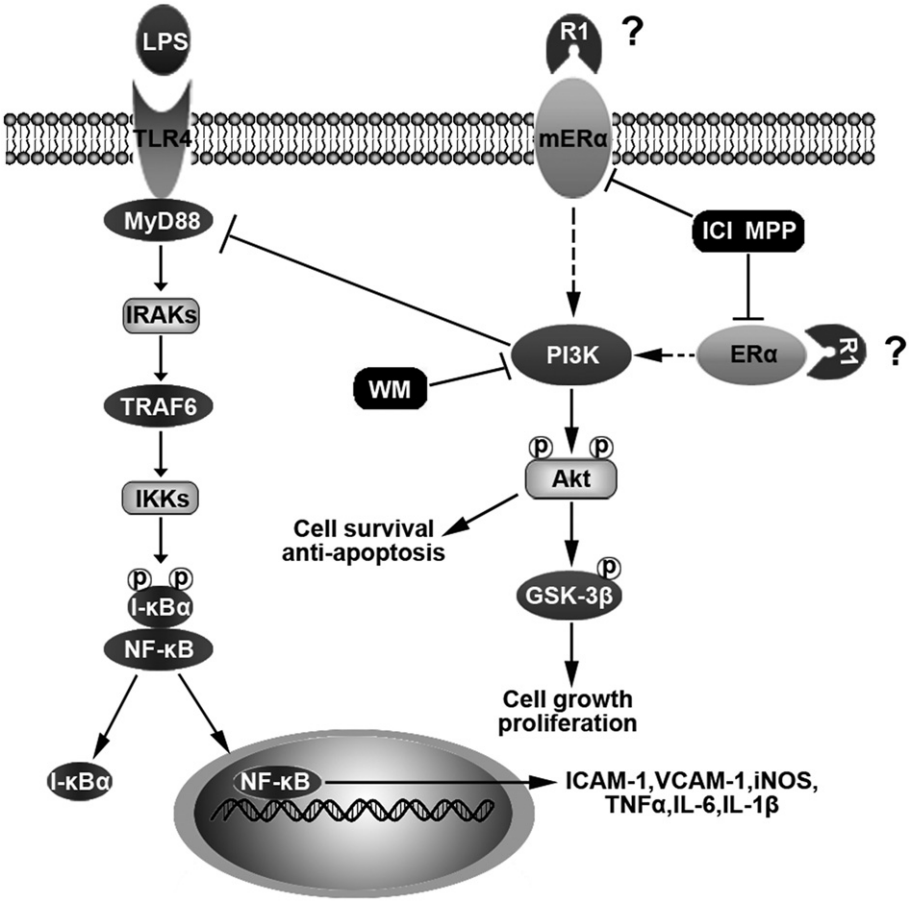

Figure 6

Scheme of mechanisms underlying attenuation of cardiac dysfunction induced by endotoxin, after NG-R1 treatment. The transmembrane TLR-4 recognizes LPS. After binding LPS, TLR-4 recruits the adaptor protein called MyD88, which interacts with IRAKs. IRAKs then interact with TRAF6, resulting in IKKs activation that causes I-κBα phosphorylation. The NF-κB then translocates to the nucleus and binds specific binding sites on DNA to stimulate the expression of inflammatory mediators, including ICAM-1, VCAM-1, iNOS, TNF-α, IL-6 and.IL-1β. NG-R1 increases the expression of ERα via unknown mechanisms. ERα activates the PI3K/Akt signalling pathway, thereby negatively regulating LPS-induced NF-κB-dependent inflammatory responses.

the phosphorylation of the p65 subunit of NF-κB and IκB-α degradation. Subsequently, the expression of its downstream pro-inflammatory genes such as TNF-α, IL-1β and IL-6 was enhanced. Importantly, NG-R1 pretreatment significantly inhibited these activities, similar to a previous report on the limited activation of NF-κB and its pro-inflammatory mediator cascade in mice following overexpression of gene encoding CCL2 (Niu *et al.*, 2011). Although the protein levels of TLR-4 were increased after LPS challenge, the up-regulated TLR-4 was not attenuated by NG-R1 pretreatment (Figure 5A). Hence, the NG-R1-induced deactivation of NF-κB and decreased inflammatory cytokine release may not be directly mediated by TLR-4.

ERs and the PI3K/Akt pathway are involved in many pathophysiological processes and play a central role in cellular survival in a variety of cell types (Schroder *et al.*, 1998; Wu *et al.*, 2005; Murphy, 2011; Xi *et al.*, 2012). The nuclear localization and activity of phospho-Akt in the myocardium is higher in females than in age-matched men (Camper-Kirby *et al.*, 2001). 17β-Oestradiol can activate Akt, resulting in reduced pathological cardiac hypertrophy and heart failure (Wu *et al.*, 2005). Our present study revealed a selective induction of ERα as well as elevated protein levels of phospho-Akt and phospho-GSK3β in the myocardium following NG-R1 treatment during sepsis and septic shock. More specifically, NG-R1 activated ERα and the downstream PI3K/Akt signalling pathway, which may have negatively regulated the LPS-induced, NF-κB-dependent inflammatory responses (Figure 6). These findings were supported by the pharmacological inhibition of ERα (by ICI 182780 or MPP) or PI3K (by wortmannin) resulting in the loss of the protective effects of NG-R1 against LPS-induced cardiac dysfunction, as well as the NG-R1-preserved phospho-Akt, phospho-GSK-3β and IκB-α following LPS challenge. The data suggest that NG-R1, as a novel phytoestrogen, promotes ERα expression via an unknown mechanism (Figure 6). Collectively, the activation of ERα and the PI3K/Akt signalling pathway may play roles in limiting the LPS-induced inflammatory and apoptotic responses, ultimately suppressing the development of septic cardiac dysfunction. The effects of NG-R1 may not be limited

to its oestrogenic properties and PI3K/Akt signalling. Our results (Supporting Information Figure S3) show that NG-R1 pretreatment can also act on the ERK1/2 MAPK pathway. This result is consistent with those of previous reports, which show that NG-R1 can act on the ROS/ERK pathway and directly scavenge ROS (Zhang and Wang, 2006b).

Pretreatment with NG-R1 also prevented apoptotic damage in the myocardium. Apoptosis is recognized as a major contributor to endotoxin-induced myocardial dysfunction (Davies, 1997; McDonald *et al.*, 2000). In the present study, the increased caspase-3/-8/-9 activities and caspase-3-activated PARP cleavage observed in the LPS-treated hearts were attenuated by NG-R1. This finding can be attributed to the reduction in the myocardial inflammatory cytokines TNF-α, IL-1β, IL-6 and NO, which are believed to be critical for caspase activation in endotoxemic models (Tatsumi *et al.*, 2004; Carlson *et al.*, 2005). Our data also revealed that NG-R1 inhibited the LPS-induced expression of pro-apoptotic mediators, p53, tBid, TNF-R1 and Fas, as well as maintaining the expression of the anti-apoptotic mediator, Bcl-2. Hence, NG-R1 mediates cardiomyocyte survival by maintaining the balance between pro-apoptotic and anti-apoptotic mediators following LPS challenge. This finding is supported by the lower amount of TUNEL-positive cells, mainly inflammatory cells, in the hearts of LPS and NG-R1 co-treated mice, than in those of LPS-treated mice.

Although NG-R1 pretreatment significantly inhibited the LPS-induced cardiac dysfunction and inflammatory reactions in mice, the results cannot be translated to patients with sepsis admitted to a hospital, primarily because the current study used pre-treatment. In addition, the duration of the experiment was only 6 h, and NG-R1 did not completely prevent the adverse events associated with endotoxemia. Thus, the therapeutic functions of NG-R1 on sepsis-related mortality have yet to be determined. Several studies have also suggested the potential of NG-R1 as a treatment for cardiac dysfunction in sepsis. A previous study showed that NG-R1 reduces LPS-related lethality in mice *in vivo* (Zhang *et al.*, 1997). In this study, half of the total NG-R1 dosage was administered 1 h before the LPS, whereas the other half was administered simultaneously with LPS. In addition, NG-R1 has potential therapeutic functions because it is purified from the Chinese herb *P. notoginseng*, which has been used by traditional Chinese doctors for thousands of years as a drug to treat cardiovascular diseases and to relieve blood stasis and pain. *P. notoginseng* treatment reduced inflammatory reactions in patients and animal models and reduced the symptoms of experimental disseminated intravascular coagulation (DIC), which is a leading cause of sepsis-related mortality in hospitalized patients (Wei, 1982; Kubo *et al.*, 1984; Hao and Yang, 1986; Chen, 1987).

The effect of NG-R1 on coagulation disorders following an LPS challenge has also been studied. NG-R1 blocked the induction of plasminogen activator inhibitor 1 (PAI-1) and tissue factor (TF) following LPS, which lead to thrombogenic changes in the fibrinolytic and coagulation systems of endothelial cells that contributed to the pathogenesis of DIC after septicemia (Zhang *et al.*, 1997). Studies also showed that NG-R1 not only inhibited PAI-1 and TF induction by LPS in endothelial cells and TNF-α generation in a human whole-blood assay, but also ameliorated the LPS-induced PAI-1 response and reduced LPS-related lethality in a mouse LPS shock model (Zhang *et al.*, 1997). Thus, NG-R1 can attenuate the LPS-induced activation of the coagulation system, reduce the fibrinolytic capacity, inhibit the neutrophil/leukocyte infiltration and inflammatory reactions and prevent myocardial dysfunction during sepsis.

In summary, the present study showed that pretreatment with NG-R1 attenuated LPS-induced myocardial inflammatory cytokine production, imbalance between iNOS and eNOS, and NF-κB activation, as well as improved myocardial dysfunction during endotoxemia. The mechanisms by which NG-R1 attenuated cardiac dysfunction involve the preserved activation of ERα and the PI3K/Akt signalling pathway. These findings demonstrate the potential of NG-R1 for the treatment of endotoxin-induced cardiac dysfunction. If the therapeutic roles of NG-R1 are fully explored in patients and animal models, NG-R1 treatment could be a promising strategy for reducing the high mortality of hospitalized patients with sepsis.

Funding

This work was supported by the Key Projects of the National Science and Technology Pillar Program (2008BAI51B02 to SXB); the Chinese National S&T Special Project on Major New Drug Innovation (2012ZX09301002-001 to SXB); and the Chinese Postdoctoral Science Foundation (20110490325 to XJ).

Conflict of interest

None declared.

References

Alexander SP, Mathie A, Peters JA (2011). Guide to Receptors and Channels (GRAC), 5th edition. Br J Pharmacol 164: S1–S324.

Avlas O, Fallach R, Shainberg A, Porat E, Hochhauser E (2011). Toll-like receptor 4 stimulation initiates an inflammatory response that decreases cardiomyocyte contractility. Antioxid Redox Signal 15: 1895–1909.

Babior BM (1999). NADPH oxidase: an update. Blood 93: 1464–1476.

Baumgarten G, Knuefermann P, Schuhmacher G, Vervolgyi V, von Rappard J, Dreiner U *et al.* (2006). Toll-like receptor 4, nitric oxide, and myocardial depression in endotoxemia. Shock 25: 43–49.

Camper-Kirby D, Welch S, Walker A, Shiraishi I, Setchell KD, Schaefer E *et al.* (2001). Myocardial akt activation and gender: increased nuclear activity in females versus males. Circ Res 88: 1020–1027.

Carlson DL, Willis MS, White DJ, Horton JW, Giroir BP (2005). Tumor necrosis factor-alpha-induced caspase activation mediates endotoxin-related cardiac dysfunction. Crit Care Med 33: 1021–1028.

Chen QS (1987). [Pharmacological studies on notoginseng saponins isolated from the fibrous root of Panax notoginseng]. Zhong Yao Tong Bao 12: 45–47.

Chen WX, Wang F, Liu YY, Zeng QJ, Sun K, Xue X *et al*. (2008). Effect of notoginsenoside R1 on hepatic microcirculation disturbance induced by gut ischemia and reperfusion. World J Gastroenterol 14: 29–37.

Court O, Kumar A, Parrillo JE (2002). Clinical review: myocardial depression in sepsis and septic shock. Crit Care 6: 500–508.

Davani EY, Boyd JH, Dorscheid DR, Wang Y, Meredith A, Chau E *et al*. (2006). Cardiac ICAM-1 mediates leukocyte-dependent decreased ventricular contractility in endotoxemic mice. Cardiovasc Res 72: 134–142.

Davies MJ (1997). Apoptosis in cardiovascular disease. Heart 77: 498–501.

Davis AM, Mao J, Naz B, Kohl JA, Rosenfeld CS (2008). Comparative effects of estradiol, methyl-piperidino-pyrazole, raloxifene, and ICI 182 780 on gene expression in the murine uterus. J Mol Endocrinol 41: 205–217.

Frangogiannis NG, Lindsey ML, Michael LH, Youker KA, Bressler RB, Mendoza LH *et al*. (1998). Resident cardiac mast cells degranulate and release preformed TNF-alpha, initiating the cytokine cascade in experimental canine myocardial ischemia/reperfusion. Circulation 98: 699–710.

Hale SL, Birnbaum Y, Kloner RA (1997). Estradiol, administered acutely, protects ischemic myocardium in both female and male rabbits. J Cardiovasc Pharmacol Ther 2: 47–52.

Hao CQ, Yang F (1986). [Anti-inflammatory effects of total saponins of Panax notoginseng]. Zhongguo Yao Li Xue Bao 7: 252–255.

Hara M, Matsumori A, Ono K, Kido H, Hwang MW, Miyamoto T *et al*. (1999). Mast cells cause apoptosis of cardiomyocytes and proliferation of other intramyocardial cells in vitro. Circulation 100: 1443–1449.

Jolly SR, Abrams GD, Romson JL, Bailie MB, Lucchesi BR (1982). Effects of lodoxamide on ischemic reperfused myocardium. J Cardiovasc Pharmacol 4: 441–448.

Kawai T, Akira S (2007). Signaling to NF-kappaB by Toll-like receptors. Trends Mol Med 13: 460–469.

Kilkenny C, Browne W, Cuthill IC, Emerson M, Altman DG (2010). NC3Rs Reporting Guidelines Working Group. Br J Pharmacol 160: 1577–1579.

Kubo M, Matsuda R, Matsuda H, Arichi S (1984). [Effect of Panax notoginseng on experimental disseminated intravascular coagulation (DIC)]. Yakugaku Zasshi 104: 757–762.

Lei XL, Chiou GC (1986). Cardiovascular pharmacology of Panax notoginseng (Burk) F.H. Chen and salvia miltiorrhiza. Am J Chin Med 14: 145–152.

Li XQ, Cao W, Li T, Zeng AG, Hao LL, Zhang XN *et al*. (2009). Amlodipine inhibits TNF-alpha production and attenuates cardiac dysfunction induced by lipopolysaccharide involving PI3K/Akt pathway. Int Immunopharmacol 9: 1032–1041.

Liu WJ, Tang HT, Jia YT, Ma B, Fu JF, Wang Y *et al*. (2010). Notoginsenoside R1 attenuates renal ischemia-reperfusion injury in rats. Shock 34: 314–320.

McDonald TE, Grinman MN, Carthy CM, Walley KR (2000). Endotoxin infusion in rats induces apoptotic and survival pathways in hearts. Am J Physiol Heart Circ Physiol 279: H2053–H2061.

McGrath J, Drummond G, McLachlan E, Kilkenny C, Wainwright C (2010). Guidelines for reporting experiments involving animals: the ARRIVE guidelines. Br J Pharmacol 160: 1573–1576.

Mallen-St Clair J, Pham CT, Villalta SA, Caughey GH, Wolters PJ (2004). Mast cell dipeptidyl peptidase I mediates survival from sepsis. J Clin Invest 113: 628–634.

Merx MW, Weber C (2007). Sepsis and the heart. Circulation 116: 793–802.

Muller WA (2009). Mechanisms of transendothelial migration of leukocytes. Circ Res 105: 223–230.

Murphy E (2011). Estrogen signaling and cardiovascular disease. Circ Res 109: 687–696.

Narula J, Kolodgie FD, Virmani R (2000). Apoptosis and cardiomyopathy. Curr Opin Cardiol 15: 183–188.

Niu J, Azfer A, Kolattukudy PE (2008). Protection against lipopolysaccharide-induced myocardial dysfunction in mice by cardiac-specific expression of soluble Fas. J Mol Cell Cardiol 44: 160–169.

Niu J, Wang K, Graham S, Azfer A, Kolattukudy PE (2011). Mcp-1-induced protein attenuates endotoxin-induced myocardial dysfunction by suppressing cardiac NF-small ka, CyrillicB activation via inhibition of Ismall ka, CyrillicB kinase activation. J Mol Cell Cardiol 51: 177–186.

Rudiger A, Singer M (2007). Mechanisms of sepsis-induced cardiac dysfunction. Crit Care Med 35: 1599–1608.

Saraiva M, O'Garra A (2010). The regulation of IL-10 production by immune cells. Nat Rev Immunol 10: 170–181.

Schroder J, Kahlke V, Staubach KH, Zabel P, Stuber F (1998). Gender differences in human sepsis. Arch Surg 133: 1200–1205.

Sun K, Wang CS, Guo J, Horie Y, Fang SP, Wang F *et al*. (2007). Protective effects of ginsenoside Rb1, ginsenoside Rg1, and notoginsenoside R1 on lipopolysaccharide-induced microcirculatory disturbance in rat mesentery. Life Sci 81: 509–518.

Tarin C, Lavin B, Gomez M, Saura M, Diez-Juan A, Zaragoza C (2011). The extracellular matrix metalloproteinase inducer emmprin is a target of nitric oxide in myocardial ischemia/reperfusion. Free Radic Biol Med 51: 387–395.

Tatsumi T, Akashi K, Keira N, Matoba S, Mano A, Shiraishi J *et al*. (2004). Cytokine-induced nitric oxide inhibits mitochondrial energy production and induces myocardial dysfunction in endotoxin-treated rat hearts. J Mol Cell Cardiol 37: 775–784.

Valsecchi AE, Franchi S, Panerai AE, Sacerdote P, Trovato AE, Colleoni M (2008). Genistein, a natural phytoestrogen from soy, relieves neuropathic pain following chronic constriction sciatic nerve injury in mice: anti-inflammatory and antioxidant activity. J Neurochem 107: 230–240.

Wei BH (1982). [Treatment of shock with traditional Chinese medicine and Western medicine]. Zhong Xi Yi Jie He Za Zhi 2: 243–196.

Wencker D, Chandra M, Nguyen K, Miao W, Garantziotis S, Factor SM *et al*. (2003). A mechanistic role for cardiac myocyte apoptosis in heart failure. J Clin Invest 111: 1497–1504.

Wu CH, Liu JY, Wu JP, Hsieh YH, Liu CJ, Hwang JM *et al*. (2005). 17beta-estradiol reduces cardiac hypertrophy mediated through the up-regulation of PI3K/Akt and the suppression of calcineurin/NF-AT3 signaling pathways in rats. Life Sci 78: 347–356.

Xi YD, Yu HL, Ding J, Ma WW, Yuan LH, Feng JF *et al*. (2012). Flavonoids protect cerebrovascular endothelial cells through Nrf2 and PI3K from beta-amyloid peptide-induced oxidative damage. Curr Neurovasc Res 9: 32–41.

Xiao J, Sun B, Cai GP (2010). Transient expression of interferon-inducible p204 in the early stage is required for adipogenesis in 3t3-l1 cells. Endocrinology 151: 3141–3153.

Xiao J, Sun GB, Sun B, Wu Y, He L, Wang X *et al.* (2012). Kaempferol protects against doxorubicin-induced cardiotoxicity in vivo and in vitro. Toxicology 292: 53–62.

Yamashita T, Kawashima S, Ohashi Y, Ozaki M, Ueyama T, Ishida T *et al.* (2000). Resistance to endotoxin shock in transgenic mice overexpressing endothelial nitric oxide synthase. Circulation 101: 931–937.

Zanotti-Cavazzoni SL, Hollenberg SM (2009). Cardiac dysfunction in severe sepsis and septic shock. Curr Opin Crit Care 15: 392–397.

Zhang HS, Wang SQ (2006a). Notoginsenoside R1 from Panax notoginseng inhibits TNF-alpha-induced PAI-1 production in human aortic smooth muscle cells. Vascul Pharmacol 44: 224–230.

Zhang HS, Wang SQ (2006b). Notoginsenoside R1 inhibits TNF-alpha-induced fibronectin production in smooth muscle cells via the ROS/ERK pathway. Free Radic Biol Med 40: 1664–1674.

Zhang WJ, Wojta J, Binder BR (1997). Notoginsenoside R1 counteracts endotoxin-induced activation of endothelial cells in vitro and endotoxin-induced lethality in mice in vivo. Arterioscler Thromb Vasc Biol 17: 465–474.

Zhou H, Qian J, Li C, Li J, Zhang X, Ding Z *et al.* (2011). Attenuation of cardiac dysfunction by HSPA12B in endotoxin-induced sepsis in mice through a PI3K-dependent mechanism. Cardiovasc Res 89: 109–118.

Supporting information

Additional Supporting Information may be found in the online version of this article at the publisher's web-site:

Figure S1 Dose-dependent effects of NG-R1 on cardiac dysfunction. Mice were treated with saline or LPS (10 $mg \cdot kg^{-1}$, i.p.) with or without NG-R1 pretreatment (0 to 100 $mg \cdot kg^{-1}$, i.p.). Cardiac function was examined by echocardiography 6 h after LPS administration. Echocardiography values are expressed as the mean ± SE (n = 15 per group). *P < 0.05 versus control (Cont); $^{\#}P$ < 0.05 versus LPS-treated mice.

Figure S2 Effects of three inhibitors, ICI 182780, wortmannin and MPP, on cardiac dimensions and function without NG-R1. Mice were pretreated with a nonselective ER antagonist, ICI 182780 (ICI; 2 $mg \cdot kg^{-1}$ body weight), a selective PI3K antagonist wortmannin (WM; 1 $mg \cdot kg^{-1}$ body weight) or a selective ERα antagonist methyl piperidino-pyrazole (MPP; 2 $mg \cdot kg^{-1}$ body weight) 1 h before LPS administration. Cardiac function was examined by echocardiography 6 h after LPS administration. Echocardiography values are expressed as the mean ± SE (n = 15 per group). *P < 0.05 versus saline; $^{\#}P$ < 0.05 versus LPS-treated mice.

Figure S3 Protein levels of phospho-ERK1/2, ERK1/2, phospho-Stat3 and Stat3 in the myocardium, as determined by Western blot analysis.

Figure S4 Effects of LPS and NG-R1 on the mast cell number. Toluidine blue-positive mast cells were counted. The abscissa represents the time after LPS infusion. Quantification of the total mast cell number includes both degranulated and non-degranulated mast cells. Results are expressesd as the mean ± SE (n = 15 per group). *P < 0.05 versus Cont; $^{\#}P$ < 0.05 versus LPS-treated mice.

Table S1 Primers used for real-time RT-PCRs.